RESPONSE OF KARST AQUIFERS TO RAINFALL AND EVAPORATION, MAHARLU BASIN, IRAN

NOZAR SAMANI
Department of Geology, Shiraz University, Shiraz 71454, IRAN samani@geology.susc.ac.ir

Maharlu basin, with an approximate surface area of 4000 km², is located in the central part of Fars Province, Iran. The basin is the first candidate site for karst hydrogeology research in the country. The karstified Asmari-Jahrum Formation covers ~37% of the total surface area of the basin with huge reservoirs of karst water. To establish the relationship between rainfall and evaporation with groundwater level and spring discharge, the fluctuations of groundwater level at nine piezometric and exploration wells, discharge of two springs, rainfall records, and pan evaporation are analyzed by employing time-series techniques both in time and frequency domains. Results are presented as correlograms, variance spectra, phase diagrams, coherency diagrams and cross correlograms. A time lag of 1-3 months was found between rainfall occurrence and the response of groundwater levels and spring discharges. There is no clear relation between evaporation and groundwater level and spring discharge. Different response in different wells is due to the different path lengths of percolated water from sinking point to the water table. The time response of groundwater level and spring discharge suggests that springs are fed through a diffuse karstic flow system that is in accordance with the physical characteristics of the springs. The lag times of Pirbanow and Pol-Brengi springs are equal in response to rainfall, but zero and 1-2 months respectively, in response to groundwater level at exploration well E-17. This point, together with the high value of specific conductivity of Pol-Brengi spring, suggests that the two springs have no hydrogeologic connection. The Ghasrodasht Fault may be the cause of this separation. It is finally concluded that a combination of time series analysis/physical properties of springs and geologic evidence can provide useful information about the hydrogeology of a region prior to large-scale and expensive tests.

A groundwater level indicates the elevation at which the water is at atmospheric pressure within the aquifer. Any phenomenon that produces a change in pressure on groundwater will cause the groundwater level to vary. Differences between supply and withdrawal of groundwater cause levels to fluctuate. Rainfall, evapotranspiration, pumpage, stream flow, and spring discharge variations are closely related to groundwater levels. The mechanism of groundwater level variations by these factors and other diverse phenomena, urbanization, earthquakes, and external loads, is given by Todd (1980). Groundwater level variations in some karst aquifers are analyzed in this work.

Karst aquifers are, in general, heterogeneous in character. As a result, quantitative data obtained from selected points in the system either by pumping or by using tracer dyes can be rarely extrapolated to evaluate the average function of the system as a whole. In contrast, analysis of groundwater level and spring discharge variations and related hydrologic controls (e.g., precipitation, evaporation) can reflect overall response of the aquifer and help in evaluating its storage, drainage potential, degree of karstification, hydrogeologic boundaries, etc., without imposing any external stresses on the system. Spring hydrograph recession curves may also be used to define the degree of karstification and conduit/diffuse flow regimes in karst aquifers (Padilla *et al.* 1994; Samani & Ebrahimi 1996). In this paper, an attempt has been made to determine whether the existing record of natural groundwater level variation could yield information on the hydrogeology of the Maharlu karst basin situated in Fars Province of Iran prior to large-scale tests. For this purpose, time-series techniques are used and the following thirteen sets of data (Sahraie 1995; Tamab 1993) are analyzed (Fig. 1):

a) monthly rainfall (cumulative rainfall depth of all rainfall events during each month) monitored at Shiraz Airport and Doboneh stations;
b) monthly pan evaporation (cumulative evaporation during a month) at the above stations;
c) monthly groundwater level at three piezometers and four exploration wells;
d) instantaneous monthly discharge of Pirbanow and Pol-Brengi springs.

All data sets extend for 7 years from October 1987 to September 1994. Figure 2 is the geological map of the Maharlu basin and shows the location of meteorological stations, piezometers, exploration wells and springs. Note from table 3 that piezometers are wells of small diameter (101 mm) with high depth (>400m) and exploration wells are shallower, large diameter wells (300-360 mm). Methods of investigation began with the application of various time-series techniques and geologic evidence and physical properties of springs are used to test the inference drawn from the time series analysis.

GEOLOGY AND HYDROGEOLOGY OF THE BASIN

Maharlu karst basin has an approximate surface area of 4000 km² and is located in the central part of Fars Province,

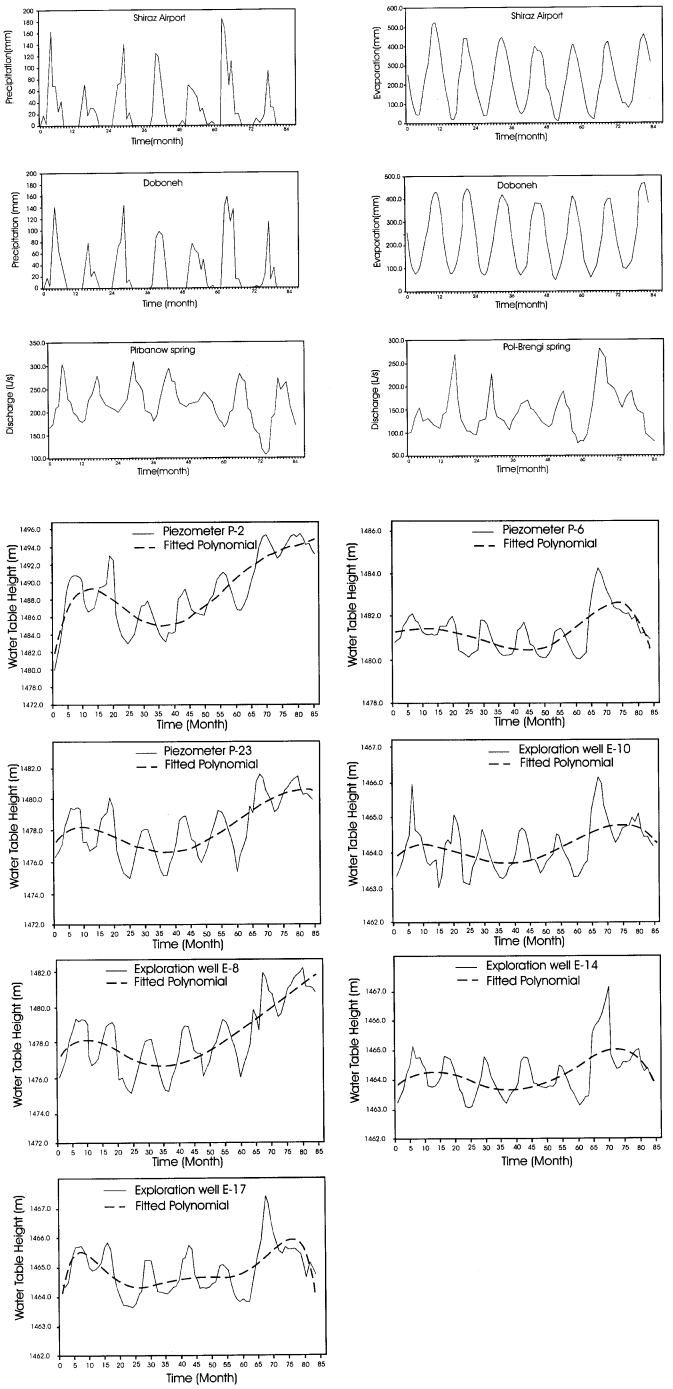

Figure 1. Raw data.

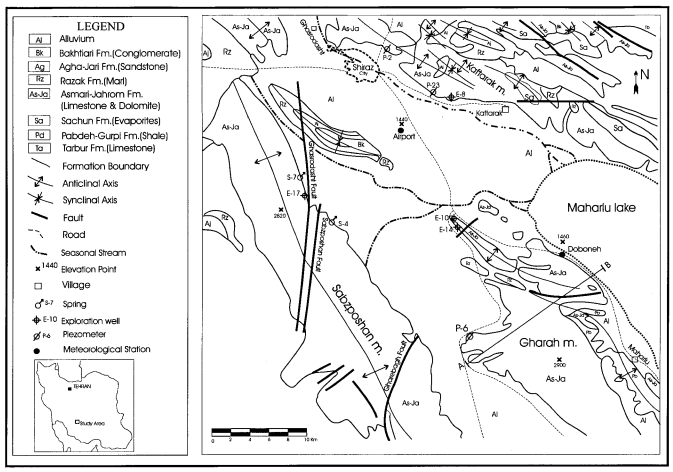

Figure 2. Geological map of Maharlu basin, location of springs, piezometers and exploration wells and meteorological stations.

Iran (29°1'30"N, 52°12'28"E). The basin falls in zone three (simple folded belt) of the Zagros Orogenic Belt. The exposed geologic formations in decreasing order of age consist of Pabdeh-Gurpi shales and gypsiferous marls (Santonian-Oligocene), Sachun gypsum (Paleocene-L.Eocene), Asmari-Jahrum limestones and dolomites (Paleocene-Oligocene), Razak evaporites (Oligocene-Miocene), Aghajari sandstone (Miocene-Pliocene), and Bakhtiari conglomerates (Pliocene) (Fig. 2). James and Wynd (1965) give the detailed lithology of these formations. The karstified Asmari-Jahrum Formation is exposed over 37% of the total surface area of the basin (Tamab 1993), forming three huge reservoirs of karst water in the Gharah, Kaftarak, and Sabzposhan anticlines. The overall trend of these anticlines follows the general NW-SE trend of the Zagros Orogeny.

Sabzposhan anticline, in the south of the basin, is crossed by three major faults and many minor ones. The major faults are the Ghasrodasht, Sabzposhan, and Gharebagh faults (Fig. 2). Pirbanow (S-4) and Pol-brengi (S-7) springs drain the Sabzposhan aquifer. The exploration well E-17 penetrates this aquifer. Tables 1 and 2 summarize the statistics for some of the physical parameters of Pirbanow and Pol-Brengi springs (Sahraei 1995).

The Kaftarak anticline, in the north of the basin, is crossed by a major fault whose hydrogeologic role is not known. The exploration well E-8 and the piezometric wells P-2 and P-23 penetrate the karst aquifer in the south flank of this anticline. Gharah anticline forms the third karst aquifer studied in this paper. The exploration wells E-14 and E-10 and the piezometric well P-6 are located in the Gharah aquifer. Some specifications of all the wells are presented in table 3.

The climate is semi-arid, with an average annual precipitation over the basin of about 350 mm. Rainfall infiltrates through karst formations to the impermeable cores (Gurpi Formation) of the anticlines. The Razak Formation behaves as an aquitard and segregates the groundwater of the karst aquifers from that of the alluvial aquifers in the basin.

METHODOLOGY

The statistical methods for analyzing time series are well established (Jenkins & Watts 1968; Chow 1978; Yevjeich 1982; Chatfield 1982; Salas *et al*. 1988). This paper focuses on

Table 1. Physical parameters of Pirbanow spring (S-7).

Parameter	Minimum	Maximum	Mean	Standard deviation	Coefficient of variation%
Discharge (L/s)	107.00	311.00	216.76	39.59	18.35
EC (µS/cm)	647.00	762.00	708.86	39.76	5.61
Water temperature (°C)	18.00	22.00	19.80	1.04	5.24
Air temperature (°C)	4.89	28.98	16.88	7.93	47.00

Table 2. Physical parameters of Pol-Brengi spring (S-4).

Parameter	Minimum	Maximum	Mean	Standard deviation	Coefficient of variation%
Discharge (L/s)	75.00	282.00	144.55	44.92	31.08
EC (µS/cm)	1190.00	1693.00	1437.00	126.21	8.78
Water temperature (°C)	19.00	23.00	20.83	1.10	5.29
Air temperature (°C)	4.89	28.98	16.88	7.93	47.00

Table 3. Some specifications of wells, elevations are from m.s.l (Tamab 1993).

Well no.	Elevation of of well site (m)	Mean elevation of GWL* (m)	Mean depth to GWL (m)	Depth of well (m)	Diameter (mm)	Casing depth
E-8	1509.2	1478.5	30.70	177	300	105
E-10	1474.43	1464.24	10.19	186	360	12
E-14	1513.32	1464.25	49.07	187	360	135
E-17	1527.87	1484.55	43.32	174	300	50
P-2	1562.49	1489.77	72.72	500	101	99
P-6	1489.04	1481.43	7.61	400	101	70
P-23	1512.62	1478.54	34.08	400	101	48

*Groundwater level

the methods of analyzing a single time series (univariate) as well as a double time series (bivariate). The traditional method for analyzing a univariate time series involves isolating the deterministic (trend and periodic) components and stochastic components. The stochastic components may then be explained in terms of stochastic models such as moving-average or autoregressive models. It is often the case in hydrology that a variable proceeds the other variable in time, like peak rainfall intensity proceeding the peak runoff discharge. In such cases bivariate time series techniques may be used to examine the relationship between two time series. A brief summary of the methods used to screen the components of a single time series is first discussed and then the methods for examining the relationship between two time series are followed.

TREND

The presence of trend or long-term fluctuations can be easily distinguished by inspection of annual mean against the sample mean. Other procedures, such as weighted moving average, differencing, and curve fitting may also be used. Figure 1 illustrates the polynomials fitted to the water level in wells and discharge at springs and table 4 shows the values of coefficients in the polynomials. In this table and in table 5, symbols E, P, and S denote exploration well, piezometer, and spring, respectively. Of thirteen time series considered, coefficients of polynomials fitted to the rainfall and evaporation time series (in both stations) were not statistically significant and, therefore, not included in table 4.

PERIODICITY

To inspect the presence of periodic components, among which seasonality is the most important, two diagnostic tools are the correlogram and power spectrum in time and frequency domains.

The correlogram is a graphical representation of serial-correlation coefficient r(k) as a function of lag k, where the values of r(k) are plotted as ordinates against their respective values of k. The serial correlation coefficients of lag k are calculated by (Chatfield 1982):

$$r(k) = \frac{C(k)}{C(0)} \tag{1}$$

Where C(k) is the auto covariance of a sample of N values of X with an estimated mean $\overline{X}$ at lag k, that is:

$$C(k) = \frac{1}{N}\sum_{t=1}^{N-k}(X_t - \overline{X})(X_{t+1} - \overline{X})$$

and C(0) is the estimation of the variance of the process as follows:

$$C(0) = \frac{1}{N}\sum_{t=1}^{N}(X_t - \overline{X})^2$$

As an example correlograms of rainfall and evaporation in Doboneh station are shown in figure 3a, and those of water level at piezometer P-6 and Pirbanow spring discharge (S-4) are shown in figure 3b.

Correlograms for all the time series analyzed show oscillations with negligible damping, thus revealing the presence of a periodic component in the total data set.

The spectrum can help determine the periods of the harmonic components in a time series. It is a plot of the spectral density S(f) against frequency f. In the case of an infinite series, Jenkins and Watts (1968) show that the spectral density is:

Table 4. Coefficients of polynomials fitted to time series.

well or spring	order of polynomial	a_0	a_1	a_2	a_3	a_4	a_5	a_6	r^2
E-8	5	1476.93	0.295	-0.023	6.15 E-04	-6.4 E-06	2.37 E-08		0.679
E-10	4	1463.82	0.088	-.006	1.00 E-04	-7.7 E-07			0.411
E-14	5	1463.76	0.095	-0.0051	5.59 E-05	5.7E-07	8.12 E-09		0.436
E-17	6	1483.81	0.311	-0.034	1.50 E-03	-3.1-E-05	3.21 E-07	-1.25 E-09	0.548
P-2	5	1480.10	1.822	-0.121	3.05 E-03	-3.2 E-05	1.25 E-07		0.742
P-6	5	1481.35	-0.007	-0.004	-2.74 E-04	5.6 E-06	-3.52 E-08		0.755
P-23	5	1477.08	0.2732	-0.021	4.90 E-04	-4.3 E-06	1.25 E-08		0.594
S-4*	5	117.84	0.3225	0.291	-1.68 E-02	3.1 E-04	-1.83 E-06		0.381
S-7**	4	219.53	-2.224	0.219	-5.24 E-03	3.5 E-05			0.695

* Pol-Brengi spring, r^2 is coefficient of correlation
** Pirbanow spring

$$S(f) = \int_{-\infty}^{+\infty} C(i) \cos 2\pi fi\,\delta \tag{2}$$

and for a finite series:

$$S(f) = \frac{1}{n}\left[C(0) + 2\sum_{i=1}^{n-1} C(i).\cos\frac{\pi ki}{n} + C(n).\cos\pi k\right] \tag{3}$$

Where frequency $f = k/2n\delta_i$, n=maximum number of lags investigated, and δ_i is the time interval of one month. If the time series contains distinct periodic terms, the spectral density of these terms will appear as high and sharp peaks in the estimated spectrum. Figure 3 illustrates the raw or detrended data, correlograms, and spectra of four sample time series. The spectrum of all series exhibits highest peaks at 0.083 cycle per month, The sharp peak indicates a significant amount of the variance having a 12-month periodicity (annual cycle). A smaller peak with a 6-month periodicity is also observed in the rainfall series. This apparently reflects the influence of the regular annual variations implied in the climatic condition of the region. Rainfall records show an obvious division of rainfall occurrence throughout the year, with the bulk of rainfall occurring from mid-fall to mid-spring, while the rest of the year is almost rainless.

The methods for examining the relationship between two time series are cross correlation and cross-spectrum functions in time and in frequency domain, as follows:

CROSS-CORRELATION FUNCTION

The cross-correlation function $r_{xy}(k)$ is defined as (Chatfield 1982):

$$r_{xy}(k) = \frac{C_{xy}(k)}{\sqrt{C_{xx}(0) \times C_{yy}(0)}} \tag{4}$$

Table 5. Cross-correlation coefficient and lag-time response of groundwater level and spring discharge to rainfall.

Rainfall	A	D	D	A	A	D	A	A	A
Spring or well	E-8	E-10	E-14	E-17	P-2	P-6	P-23	S-4	S-7
Cross corr. coeff.	0.62	0.72	0.70	0.82	0.60	0.70	0.60	0.60	0.70
Lag time (month)	1-2	1-2	1-2	2-3	2-3	2	1-2	1	1

A: Airport, D: Doboneh

where

$$C_{xy}(k) = \frac{1}{N-k}\sum_{i=1}^{N-k} X_i Y_{i+k} - \frac{1}{N^2}\sum_{i=1}^{N} X_i \sum_{i=1}^{N} Y_i$$

is coefficient of cross covariance at lag k for time series X_t and Y_t, and

$$C_{xx}(0) = \frac{1}{N}\sum_{i=1}^{N} (X_i - \bar{X})^2$$

and

$$C_{yy}(0) = \frac{1}{N}\sum_{i=1}^{N} (Y_i - \bar{Y})^2$$

are variance at lag zero for the two series. The plot of $r_{xy}(k)$ against k is the cross correlogram. The maximum values of $r_{xy}(k)$ observed at a lag d indicates that one series is related to the other when delayed by time d. Figure 4 illustrates the cross correlogram of four pairs namely a) rainfall-spring discharge, b) pan evaporation-water table, c) rainfall-water table, and d) pan evaporation-spring discharge. From these figures it can be

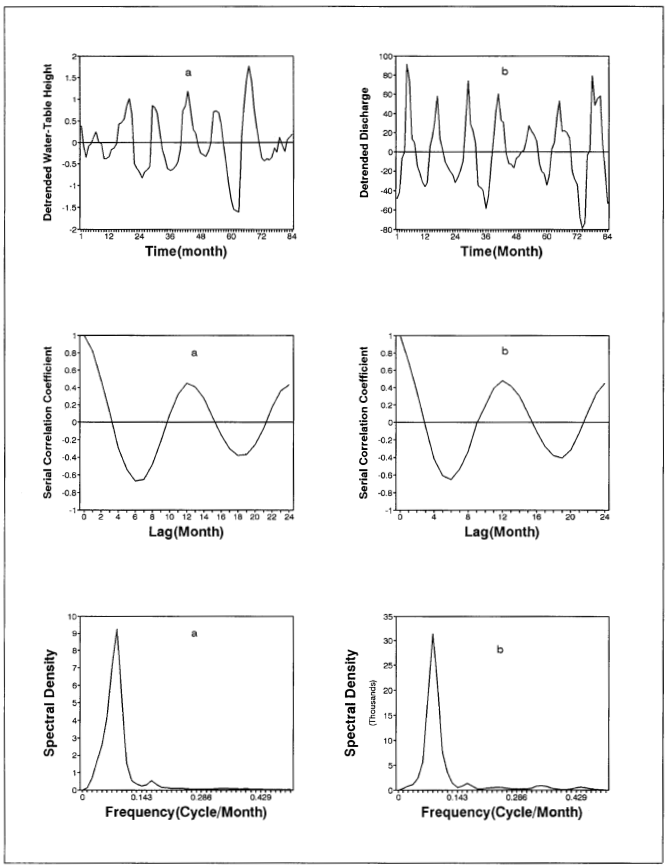

Figure 3a. Raw (or detrended) data, correlogram and spectrum. a) Groundwater level (P-6) b) Spring discharge (S-4).

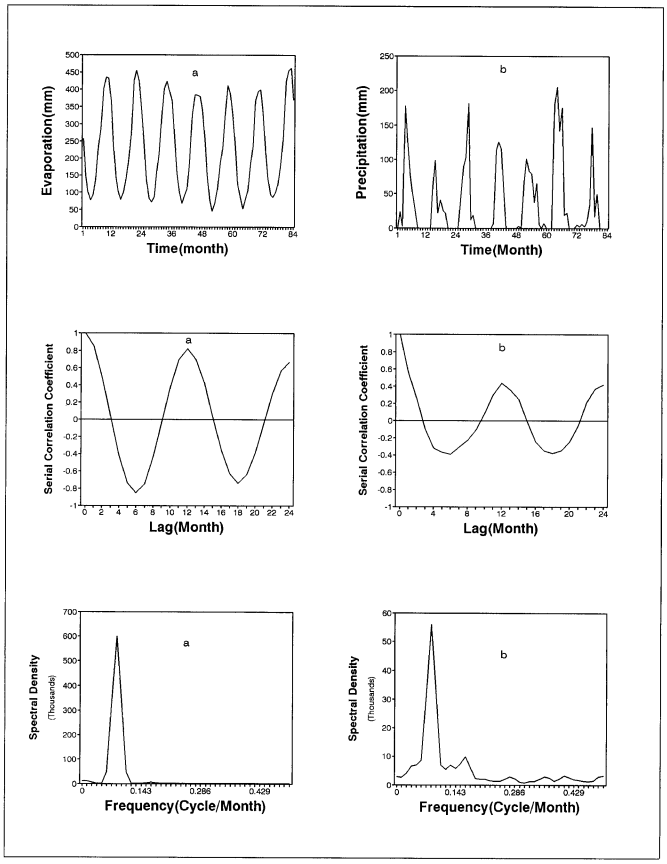

Figure 3b. Raw data, correlogram and spectrum of a) Evaporation and b) Rainfall at Doboneh station.

observed that there is no relation (i.e. no clear peak observed) between *pan evaporation-water table* and *pan evaporation-spring discharge* pair series, however there is a month lag between *rainfall-spring discharge* and a two-month lag between *rainfall-water table*. Table 5 summarizes the maximum value of $r_{xy}(k)$ and corresponding lag time for the related series.

CROSS- SPECTRUM FUNCTION

The cross spectrum function is the Fourier transform of the cross covariance. Various functions may be derived from the cross spectrum among which the coherence and phase spectra are used in this paper. The coherence spectrum is defined as:

$$Ch_{xy}(f) = \frac{C_{xy}^2(f) + q_{xy}^2(f)}{S_x(f) \times S_y(f)} \qquad (5)$$

in which $Ch_{xy}(f)$ is the coherence spectrum in frequency domain,

$$q_{xy}(f) = \frac{1}{\pi}\left[\sum_{k=1}^{\infty}\left[C_{xy}(k) - C_{yx}(k)\right]\right]\sin fk$$

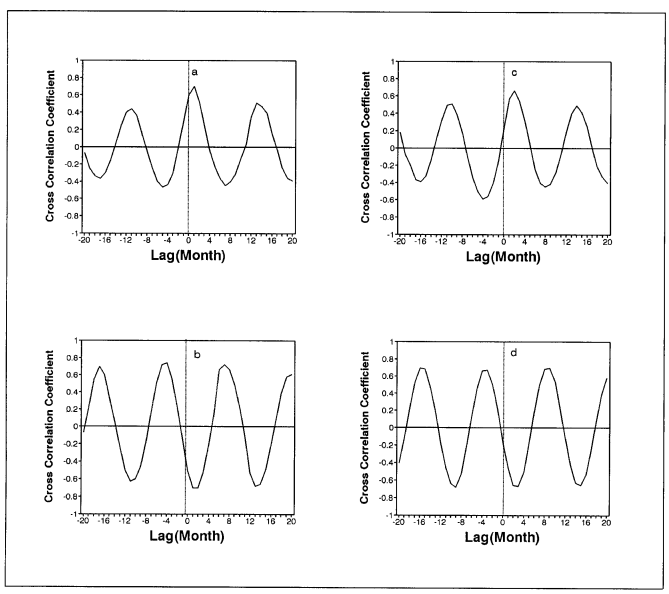

Figure 4. Cross correlograms: a) Rainfall (Airport)-spring discharge (Pirbanow), b) Evaporation (Airport)-spring discharge (Pirbanow), c) Rainfall (Doboneh)-groundwater level (P-6), and d) Evaporation (Doboneh)-groundwater level (P-6).

is the quadrature spectrum, and

$$C_{xy}(f) = \frac{1}{\pi}\left[C_{xy}(0) + \sum_{k=1}^{\infty}\left[C_{xy}(k) + C_{yx}(k)\right]\right]\cos fk$$

is the co-spectrum, and $S_x(f)$ and $S_y(f)$ are spectral densities of time series X_t and Y_t, respectively (Eq. 3). The plot of coherence spectrum against frequency is the coherency diagram. The values of Ch_{xy} vary between unity and zero, where unity indicates that the two series are fully dependent and zero shows two independent series (Chow 1978; Granger & Hatanaka 1964).

The phase spectrum determines the time lag between the two series and defined as:

$$P_{xy}(f) = \arctan\left[\frac{q_{xy}(f)}{C_{xy}(f)}\right] \qquad (6)$$

Where

$$q_{xy}(f) = \frac{1}{\pi}\left[\sum_{k=1}^{\infty}\left[C_{xy}(k) - C_{yx}(k)\right]\right]\sin fk$$

The plot of $P_{xy}(f)$ against f is the phase diagram. On the phase diagram, the frequency at which coherence is maximum gives the phase between the two series. In turn, division of phase by angular frequency gives the lag between the two series. This time lag may be compared with that found from the cross correlogram, table 5. As an example, coherence and phase diagrams for the four pair series of rainfall-water table, rainfall-spring discharge, evaporation-water table and evaporation-spring discharge are shown in figure 5. Maximum coherency and phase between these series are noted on these figures and listed in table 6. The values in the sixth column are calculated from $k = \theta T/2\pi$, where k is the time lag, θ angular frequency, and T is period.

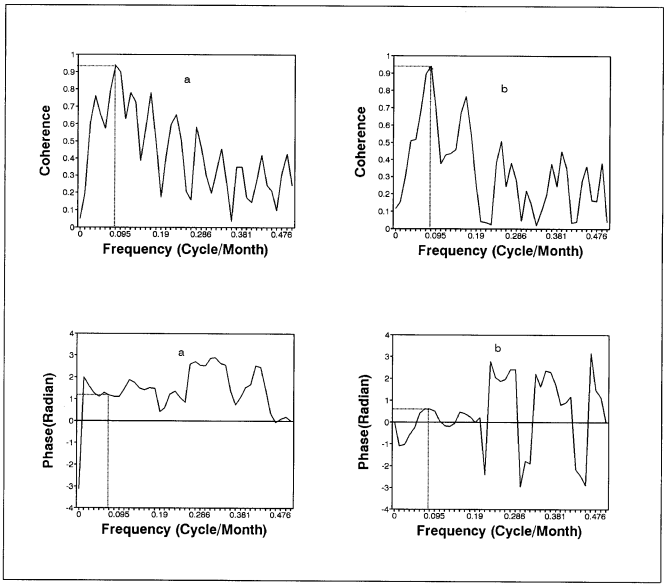

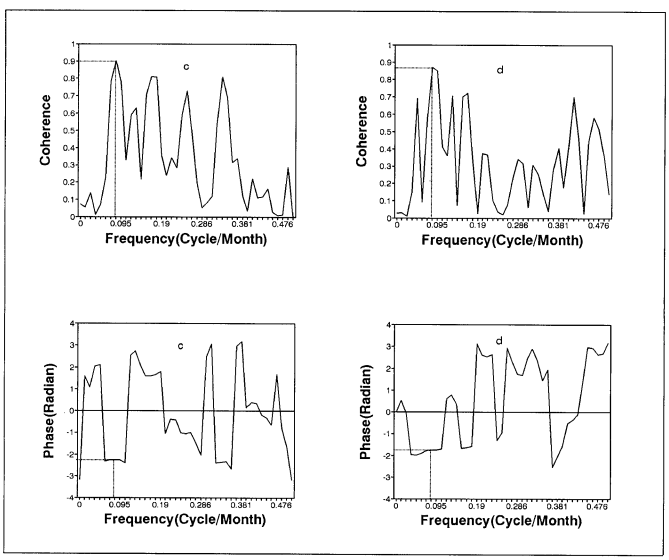

Figure 5. Coherency and phase diagrams:
a) Rainfall(Airport)-groundwater level(P-6)
b) Rainfall(Airport)-spring discharge(S-4).
c) Evaporation(Airport)-spring discharge(S-4), and
d) Evaporation(Doboneh)-groundwater level(P-6).

DISCUSSION

The time series analyses conducted in this study show that a time lag of one to three months exists between rainfall occurrence and both the groundwater level response and spring discharge, whereas there is no significant relation between evaporation and groundwater level or spring discharge (see Figs. 3b and 3d). To draw some conclusions about the hydrogeology of the karst basin from these analyses the following discussion is pertinent.

The response time of the groundwater level and spring discharge to rainfall gives some indication of the degree of karstification, type of flow regime, and the drainage/transmission and storage potential of a karst aquifer. A short time response of less than 10-15 days, or a long time response of more than 2 months, corresponds to high and low degree of karstification, respectively (Obarti *et al.* 1988). A high degree of karstification reflects development of speleological features, like sinkholes, interconnected caves, and solution channels. As a result, a well-karstified aquifer is characterized by high drainage potential, high transmissivity, and turbulent type of flow within conduits. Groundwater response at all the studied sites shows a lag time of 1-2 months. From this it may be concluded that the studied karst systems are intermediate class between high and low karstification, according to Obarti's

Table 6. Time lag response of groundwater level and spring discharge to rainfall based on cross-spectrum analysis.

well or spring	greatest coherency, $Ch_{xy}(f)_{max}$	Frequency, f (cycles/month)	Period $1/f$ (month)	Phase, θ (radian)	lag (month)
E-8	0.94	0.083	12	0.94	1.8
E-10	0.94	0.083	12	0.84	1.6
E-14	0.95	0.083	12	0.84	1.6
E-17	0.89	0.083	12	1.09	2.1
P-2	0.94	0.083	12	1.09	2.1
P-6	0.94	0.083	12	1.09	2.1
P-23	0.96	0.083	12	0.94	1.8
S-4	0.93	0.083	12	0.48	0.9
S-7	0.95	0.083	12	0.60	1.1

classification. Higher frequency data (i.e. weekly or daily) are needed for the identification of highly karstified systems with conduit flow. But for the case of our karst system, based on weekly data, Samani and Ebrahimi (1996) analyzed the recession curves of the spring hydrographs. They reported that the discharge of both Pirbanow and Pol-Brengi springs consists of 90% diffuse and 10% conduit flow.

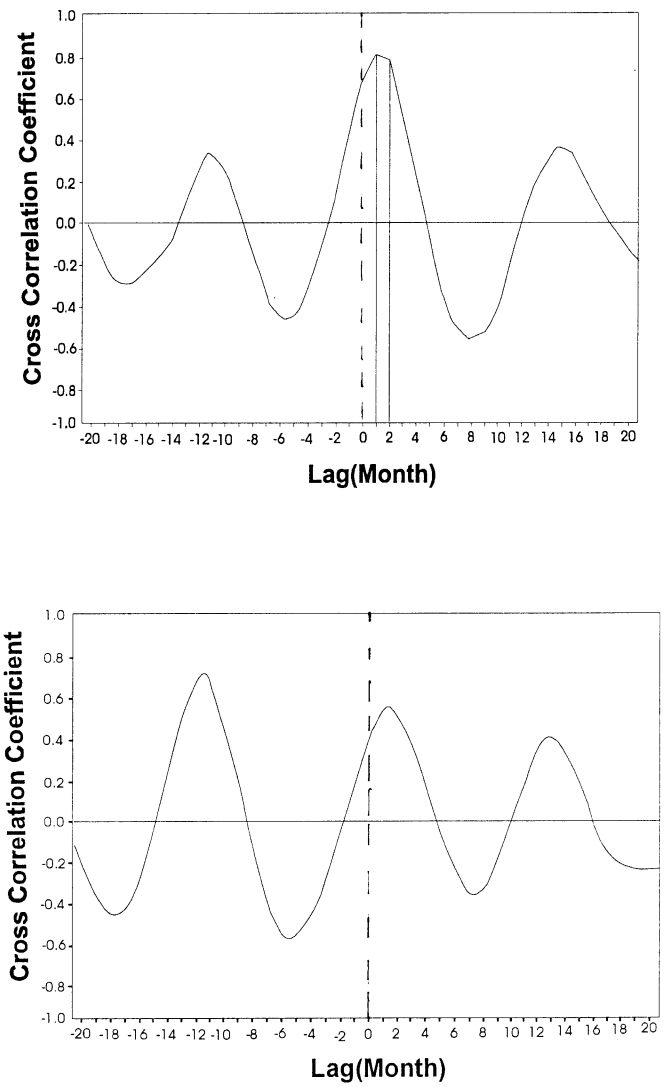

Figure 6. Cross correlograms: a- (E-17 and S-4), and b- (E-17 and S-7).

On the basis of statistical parameters of the physical characteristics of the two springs (Tables 1 & 2), and with reference to Jacobson and Langmuir (1974), the flow regime in the karst system feeding Pirbanow spring is of diffuse type. Similarly, and with the exception of high values of EC (more than 600 $\mu S/cm$, i.e., the upper limit given by Jacobson and Langmuir, 1974), the flow regime in the system feeding Pol-Brengi spring is also of diffuse type. Both springs emerge from the Sabzposhan anticline and the lag-time responses (residence times of the infiltrated rainfall in the karst system) of both springs are close to each other, therefore the flow regime of their respective karst system is diffuse. It is logical to consider Sabzposhan aquifer as a single hydrogeological unit. However, the high value of EC for Pol-Brengi spring (1190-1693 $\mu S/cm$) refutes this conclusion. To substantiate this the cross correlation coefficient between the springs and water levels at exploration well E17 were computed. A lag time of 1-2 month exists between Pirbanow spring discharge and the groundwater level at exploration well E-17 (Fig. 6a), but Pol-Brengi discharge is totally independent of groundwater level variations at exploration well E17 (Fig. 6b). In other words there is no connection between Pol-Brengi spring and exploration well E-17, and they are not fed by the same aquifer. This, together with the high value of EC and the fact that Pol-Brengi spring is 2 km further away from E-17 compared to Pirbanow spring, imply that Sabzposhan aquifer consists of two hydrogeological units, the North Sabzposhan unit drained by Pirbanow and the South Sabzposhan unit drained by Pol-Brengi spring. It seems that the Ghasrodasht fault is the cause of this separation that brings lower shaly and gypsiferous marly Pabdeh-Gurpi Formation in contact with karst water and, hence, increases EC value of Pol-Brengi and creates a groundwater barrier between two units (see Fig. 2).

In order to interpret different lags of water level-rainfall in different wells, well logs were examined and depth to water table or the water percolation path from ground surface to the water table for each well was estimated. Table 3 summarizes the mean elevation and depth of groundwater level in all the wells.

Groundwater level variations at wells P-2, P-23, and E-8 penetrating into the Kaftarak aquifer show the same patterns (see Fig. 1). Visual inspection of their logs indicates similar lithology and structural features, in terms of porosity and fractures density (Sahraie 1995). The mean depth of groundwater level at P-2, P-23 and E-8 is 72.72 m, 34.08 m and 30.70 m, respectively (Table 3). The time lag response of E-8 and P-23 with respect to rainfall is 1.8 month and that of P-2 is, however, somewhat longer, i.e. (2.1 months) (Table 6). From this comparison it seems logical to assume the longer time lag response of P-2 to rainfall is a result of a deeper groundwater level.

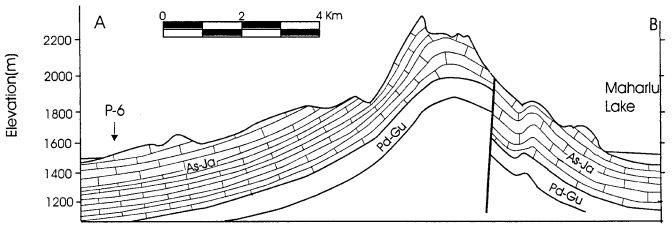

Figure 7. Geological cross section of the Gharah Anticline.

In spite of the fact that exploration wells E-10 and E-14 and piezometer P-6 penetrate into the Gharah aquifer, and the water level at P-6 is at a considerably shallower depth (7.61 m), the time lag response of P-6 is longer. Therefore, in contrast to the Kaftarak aquifer, the mean depth of water level does not control the time lag. Inspection of well logs shows no major contrast (in terms of porosity and fractures density) between them (Sahraei 1995) that would cause faster flow towards E-10 and E-14 or that would slow down flow toward P-6. Piezometer P-6 is located at the foot of the southwestern flank of the Gharah anticline and exploration wells E-10 and E-14 on the northeastern flank. Examination of the geological map and cross-section of the anticline (Figs. 2 & 7), shows that the SW flank of the anticline covers a more extensive surface area than the NE flank and the slope of the NE flank is very much steeper than that of the SW flank. From these observations it may be concluded that the mean groundwater flow path toward P-6 is longer, causing a longer time-lag response to rainfall.

CONCLUSIONS

A combination of statistical methods, physical characteristics of springs, and geologic evidence was used to study the interrelationship of groundwater level and spring discharge to rainfall and evaporation in the Maharlu karst basin. The available groundwater data were the result of several years of monitoring natural level variation at various boreholes (extending through three karst aquifer systems) and of the natural variation of discharge of two springs. Rainfall and evaporation data were taken from two meteorological stations in the basin. The combination of statistical analysis, physical properties of springs, and geologic evidence proved to be complementary in providing useful information about the hydrogeology of the study area. Groundwater levels in all the boreholes respond to rainfall but are independent of evaporation. Different lags between rainfall and water level in different boreholes are probably due to different path lengths of percolating water from sinking points to the water table. The Sabzposhan aquifer was previously believed to be a single hydrogeologic unit, but seems to consist of two separate units. The Ghasrodasht fault is the possible cause of this separation. The impermeable shaly Pabdeh-Gurpi Formation may be an impediment to groundwater flow. This type of study has several advantages: 1) lack of disturbance to the groundwater system; 2) relative simplicity in terms of the statistical method; 3) low cost associated with analysis of data from existing wells and springs.

ACKNOWLEDGMENT

This research was supported by the Iranian National Center for Scientific Research. Useful comments and suggestions given by the Associate Editor and the two anonymous reviewers are appreciated.

REFERENCES

Chatfield, C., 1982, The analysis of time series: Theory and practice: London, Chapman and Hall.

Chow, V.T., 1978, Stochastic modeling of watershed systems, Advances in Hydroscience: New York., Academic Press.

Granger, C.W.J. & Hatanaka, M., 1964, Spectral Analysis of Economic Time Series: Princeton, New Jersey, Princeton University Press.

Jacobson, R.L. & Langmuir, D., 1974, Controls on the quality variation of some carbonate spring waters: Journal of Hydrology, v. 23, p. 247-265.

James, G.A. & Wynd, J.G., 1965, Stratigraphic nomenclature of Iranian Oil Consortium Agreement Area: Bulletin of the American Association of Petroleum Geologists, v. 49, no. 12, p. 2182-2245.

Jenkins, G.M. & Watts, D.G., 1968, Spectral Analysis and its Application: San Francisco, Holden-Day Inc.

Obarti, F.J., Garay, P. & Morell, I., 1988, An attempt to karst classification in Spain based on system analysis, *in* IAH 21st Congress, Karst hydrogeology and karst environment protection, Guilin, China, p. 328-336.

Padilla, A., Pulido, A. & Mangin, A., 1994, Relative importance of baseflow and quickflow from hydrographs of karst spring: Ground Water, v. 32, no. 2, p. 267-277.

Sahraei, H., 1995, Response of karstic aquifer to hydrological factors [MS thesis]: Shiraz University, 181 p.

Salas, J.D. *et al*., 1988, Applied modeling of hydrological time series, Water Resources Publication: Fort Collins, Colorado.

Samani, N. & Ebrahimi, B., 1996, Analysis of spring hydrographs for hydrogeological evaluation of karst aquifer system: Journal of Theoretical and Applied Karstology, v. 8, p. 97-112.

Tamab, 1993, Comprehensive study and research in water resources of Maharlu karst basin (Fars): Final report, v. 1, Hydrogeology of the Basin, 284 p.

Todd, D.K., 1980, Groundwater Hydrology: New York, John Wiley and Sons, Inc.

Yevjevich, V., 1982, Stochastic processes in hydrology: Water Resources Publication, Fort Collins, Colorado.